

Combined effects of electric and magnetic fields on confined donor states in a diluted magnetic semiconductor parabolic quantum dot

A. John Peter¹, K. Gnanasekar^{2,a}, and K. Navaneethakrishnan²

¹ Zhejiang Institute of Modern Physics, Zhejiang University, Hangzhou, 310027, P.R. China

² School of Physics, Madurai-Kamaraj University, Madurai 625021, India

Received 22 May 2006

Published online 27 October 2006 – © EDP Sciences, Società Italiana di Fisica, Springer-Verlag 2006

Abstract. A variational formalism for the calculation of the binding energies of hydrogenic donors in a parabolic diluted magnetic semiconductor quantum dot is discussed. Results are obtained for $\text{Cd}_{1-x_{in}}\text{Mn}_{x_{in}}\text{Te}/\text{Cd}_{1-x_{out}}\text{Mn}_{x_{out}}\text{Te}$ structures as a function of the dot radius in the presence of external magnetic and electric fields applied along the growth axis. The donor binding energies are computed for different field strengths and for different dot radii. While the variation of impurity binding energy with dot radii and electric field are as expected, the polarizability values enhance in a magnetic field. However, for certain values of dot radii and in intense magnetic fields the polarizability variation is anomalous. This variation of polarizability is different from non-magnetic quantum well structures. Spin polaronic shifts are estimated using a mean field theory. The results show that the spin polaronic shift increases with magnetic field and decreases as the electric field and dot radius increase.

PACS. 75.50.Pp Magnetic semiconductors – 73.21.La Quantum dots – 78.67.Hc Quantum dots

1 Introduction

The fabrication of many quantum-well structures with dimensions comparable to the de Broglie wavelength is possible especially after the invention of experimental techniques such as molecular beam epitaxy, chemical vapour deposition and electron lithography. The interest in the quantum size effects present in the low dimensional structures is that they exhibit some physical properties such as optical and electronic transport characteristics which are entirely different from those of the bulk semiconductor constituents [1]. Since the electronic confinement is increased while reducing the dimensionality one can expect these characters more pronounced. The fabrication of semiconductor heterostructures with quantum confinement in all the three directions is expected to exhibit some exotic electronic behaviour.

Self-assembled quantum dots (QDs) formed in highly strained semiconductor heterostructures are a subject of considerable interest [2]. In particular, the magnetoconductance fluctuations observed in ballistic quantum dots have been the subject of intensive research in the past few years [3,4]. QDs patterned on top of two dimensional elec-

tron gases are now commonly used as an experimental tool for the investigation of a particular regime of quantum transport where the electron dynamics is both ballistic and coherent [5]. The magnetic field was usually applied perpendicular to the quantum well so as to get the maximum magnetic flux enclosed by the electron trajectories. But it has been shown that the presence of the component of the field parallel to the quantum well can strongly affect some phenomena such as magneto conductance fluctuations [6]. In the presence of magnetic field the confined hydrogenic impurities located at any position inside a semiconductor crystal have drawn considerable attention in the past few years [7,8]. Vivas-Moreno et al. [9] have calculated the binding energy of a shallow donor on-centre impurity located in cylindrical shaped GaAs-(GaAlAs) low dimensional systems, considering an infinite potential in all surfaces of the structures with the intensity of magnetic field applied in an axial direction. Recently the study of magnetic field on the ground state energy and binding energy of a hydrogen impurity within a spherical QD were studied by Maduene et al. [10]. The experimental and theoretical works on the effects of electric and magnetic fields in GaAs/Ga_{1-x}Al_xAs quantum wells have also been the subject of interest in past [11,12]. In particular, electric

^a e-mail: kgnnskr@yahoo.com

and magnetic field effects on confined donor impurities in GaAs/Ga_{1-x}Al_xAs quantum wells have been reported by Yoo et al. [13]. The influence of the different sizes on the energy levels, in the presence of magnetic and electric effects was analyzed by Ben Salem et al. [14].

In this work, we present a variational calculation of binding energies of the donor impurities in Cd_{1-x}Mn_xTe quantum dots in the presence of parallel magnetic and electric fields applied along the growth direction. We work within the effective mass approximation and adopt a variational envelope wave function for the donor electron. A systematic study with variation of magnetic and electric fields as well as dot radii has been attempted for the finite barrier confinement of a parabolic quantum dot. We also investigate theoretically the donor bound spin polaron in a quantum dot. The mean field theory with modified Brillouin function that is already used for bulk and quantum well cases has been extended to the case of a QD and we estimate the spin polaronic shifts to the impurity ionization energies. Moreover, the introduction of magnetic ions such as Mn into these compounds leads to the formation of diluted magnetic semiconductors, in which the exchange interaction between the magnetic ions and electronic states opens perspectives for interesting new phenomena. One such possibility is observing a situation in which the exchange-interaction-enhanced spin splitting of a Landau level coinciding with the energy separation between adjacent Landau levels (cyclotron energy), where interaction of the two resonances might be expected. In Section 2, we present the theoretical framework of the problem while the results and discussion are provided in Section 3. To our knowledge, this is the first calculation on a hydrogenic impurity in a parabolic diluted magnetic semiconductor quantum dot in the presence of both magnetic and electric fields.

2 Model and calculations

2.1 Ionization energy

We consider a parabolic QD (depth V_D , and radius R) of the magnetically non-uniform “spin-doping” superlattice system such as Cd_{1-x_{out}}Mn_{x_{out}}Te/Cd_{1-x_{in}}Mn_{x_{in}}Te/Cd_{1-x_{out}}Mn_{x_{out}}Te. Such a QD may be fabricated by the method of evolution of self-assembled quantum dots (QDs) in the Stransky-Krastanow mode as in the case of Cd_{1-x}Mn_xSe QDs or by electron beam lithography and wet chemical etching which is used to fabricate quantum wires [15].

In the effective mass approximation, the Hamiltonian of an electron in a parabolic QD in the presence of a magnetic field B along the z direction with the superposition of electric field F , may be written as

$$H_D = \frac{1}{2m^*} \left(\vec{p} - \frac{e\vec{A}}{c} \right)^2 + |e|Fz + V_D + H_{zee} + H_m \quad (1)$$

where $V_D = V_0(B)r^2/R^2$ for $|r| \leq R$ while $V_D = V_0(B)$ for $|r| > R$, and $V_0(B)$ is the barrier height of the

Table 1. Variation of critical field with composition.

Composition x	Critical magnetic field in Tesla	
	Expt. values for acceptors	Extrapolated values for donors
0.07	2.0 [®]	20
0.24	28.5 [#]	285
0.3	90.0 [§]	900

[®]Reference [28]; [#]reference [19]; [§]reference [29].

parabolic dot, which is taken to be 70% of the difference in the band gap between Cd_{1-x_{out}}Mn_{x_{out}}Te and Cd_{1-x_{in}}Mn_{x_{in}}Te. The barrier height decreases as the magnetic field increases as a result of variation of band offsets. In equation (1), H_{zee} and H_m refer to the interaction of electron spin with the applied field (Zeeman effect) and the interaction between electron spin and Mn²⁺ ions respectively (see Sect. 2.2).

The variation of conduction band offset with magnetic field is obtained by extrapolating the model used for the case of valence band offset variation, which incorporates the experimentally available critical magnetic fields at which a type I to type II transition occurs [16]. Assuming the other characteristics are same, the experimentally observed critical magnetic fields at which a type I to type II transition occurs, has been multiplied by a weight factor 10, because barrier height is normally taken to be 30% of the band gap differences between the layers of the heterostructure for acceptors and 70% for donors and the exchange parameters for holes and electrons are 880 meV and 220 meV respectively [17].

The variation of the band gap differences with magnetic field is given by [16]

$$\left(\frac{\Delta E_g^B}{\Delta E_g^0} \right) = \frac{\eta e^{-\varsigma\gamma} - 1}{\eta - 1} \quad (2)$$

where ΔE_g^B and ΔE_g^0 are the band gap differences with and without magnetic field respectively. $\eta = e^{\varsigma\gamma_0}$ is chosen with ς as a parameter and γ_0 as the critical field. In our calculation ς is taken to be 0.5. We define $\gamma = \hbar\omega_c/2Ry^*$ where Ry^* is the effective Rydberg (11.024 meV) and ω_c is the cyclotron frequency. The band gap of the material is given by [18] $E_g(\text{Cd}_{1-x}\text{Mn}_x\text{Te}) = 1606 + 1587x$ (meV). The variation of barrier height with magnetic field is given in Figure 1. The critical magnetic field depends upon the composition of Mn. Experimentally observed critical magnetic fields for three different compositions [19] and the extrapolated critical magnetic field for the case of donors are given in Table 1. The critical fields (in Tesla) for other values of composition can be obtained using

$$B_c = Ae^{nx}, \quad (3)$$

where $A = 0.734$ and $n = 19.082$ which gives the best fit to the extrapolated experimentally observed critical magnetic fields for $x = 0.07, 0.24$ and 0.3 . It should be noted that the barrier height depends on spin polarity and is opposite for spin-up and spin-down states.

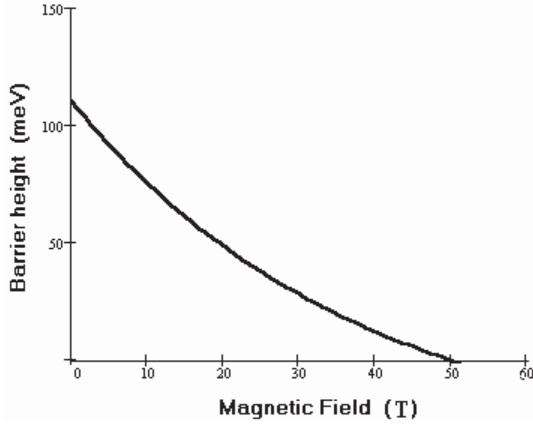


Fig. 1. Calculated barrier height for various magnetic fields for a composition $x = 0.1$.

The ground state energy of an electron in a parabolic quantum dot with magnetic and electric fields is estimated by variational method. We have assumed the trial functions as

$$\begin{aligned}\psi_{in}^{(0)}(r) &= A_{in} e^{-\xi r^2} (1 + \nu F r \cos \theta) & r < R \\ \psi_{out}^{(0)}(r) &= -A_{out} \frac{e^{-\delta r}}{r} (1 + \nu F r \cos \theta) & r \geq R.\end{aligned}\quad (4)$$

Here A_{in} and A_{out} are normalization constants. By matching the wave functions and their derivatives at the boundaries of the QD, and along with the normalization, we fix the values of A_{in} , A_{out} , and $\xi = 1/R(1/R + \delta)$. We take δ and ν as the variational parameters. By introducing the effective Rydberg $Ry^* = m^* e^4 / 2 \hbar^2 \epsilon^2$ as the unit of energy and the effective Bohr radius $a^* = \hbar^2 \epsilon / m^* e^2$ (60 Å) as the length unit, the Hamiltonian given in equation (1) becomes

$$H_D = -\nabla^2 + \frac{\gamma^2}{4} r^2 \sin^2 \theta + \gamma L_z + \frac{|e| a^* F r \cos \theta}{Ry^*} + \frac{V_D}{Ry^*} \quad (5)$$

where V_D is the parabolic confinement. In equation (5), we have dropped H_{zee} and H_m terms of equation (1), as we wish to handle them separately. In the absence of the electric field, equation (1) may also be written as, for motion along the z -direction,

$$H'_D = E_0 + \left(n + \frac{1}{2}\right) \hbar \omega_c + \mu_B g(z) S_z B + \frac{P_z^2}{2m} \quad (6)$$

where the effective g -factor is a function of the coordinate z and E_0 is the band edge energy. The effective potential for the motion in z -direction is step-like and its amplitude is determined only by the variation of the g -factor [20],

$$U = g \mu_B s_z B = x J s_z \langle S_z \rangle. \quad (7)$$

Let us consider the H_{zee} term. For an electron spin, the separation between the Zeeman levels is given by $\hbar \omega = \hbar \gamma_g B_0$ where γ_g is the gyromagnetic ratio. For $B_0 \sim 40$ Tesla, we obtain a value of ~ 5 meV for the separation. As this is small when compared to the exchange

energy, we drop the Zeeman effect. The ground state energy of the conduction electron in a parabolic QD in the external magnetic and electric fields, E_D , is obtained by minimizing the expectation value of H_D with respect to the variational parameter δ , which minimizes H_D in the absence of electric field for various magnetic fields, and ν for various electric fields using equation (4).

The Hamiltonian for a donor situated at the center of the parabolic dot in the presence of external magnetic and electric fields applied along the growth direction is

$$H_{ID} = H_D - \frac{2}{r}. \quad (8)$$

The ionization energy of the donor in the presence of magnetic and electric fields, $E_{ion}(B, F) = E_D + \gamma - \langle \psi | H_{ID} | \psi \rangle_{\min}$, is obtained by variational method using the following trial wave functions with β as the variational parameter:

$$\begin{aligned}\psi_{in}(r) &= \psi_{in}^{(0)} e^{-\beta r} & r < R \\ \psi_{out}(r) &= \psi_{out}^{(0)} e^{-\beta r} & r \geq R.\end{aligned}\quad (9)$$

2.2 Spin polaronic effect

The exchange interaction arising between the spin of a conduction electron and the Mn^{2+} spins is described by the Hamiltonian H_m as

$$H_m = - \sum J(\mathbf{r}, \mathbf{R}_j) \mathbf{s} \cdot \mathbf{S}_j. \quad (10)$$

Here \mathbf{S}_j is the spin of the Mn^{2+} ion at position \mathbf{R}_j and \mathbf{s} is the spin of the conduction electron centered at \mathbf{r} . The exchange interaction $J(\mathbf{r}, \mathbf{R}_j)$ is dependent on the overlap between the orbital of the conduction electron and of the $3d$ electrons.

Kasuya and Yanase [21], who explained the transport properties of magnetic semiconductors, originally developed the theory of spin polaron (SP). This mean field theory, which invokes the exchange interaction between the carrier and magnetic impurity in the presence of an external magnetic field B , yields the spin polaronic shift, E_{sp} , with the modified Brillouin function [17]

$$E_{sp} = \frac{1}{2} \alpha N_0 \int x S_0(x) |\psi|^2 B_s \left[\frac{S \alpha |\psi|^2}{2k_B [T + T_0(x)]} + \frac{g \mu_B S B}{k_B [T + T_0(x)]} \right] d\tau \quad (11)$$

where α is the exchange coupling parameter, S is the Mn^{2+} spin, and $x N_0$ is the Mn ion concentration. The integration is on spatial coordinates. Also $g \approx 2$, and B is the strength of the external magnetic field. $S_0(x)$, the effective spin, and $T_0(x)$, the effective temperature are the semi-phenomenological parameters, which describe the paramagnetic response of the Mn^{2+} ions in the bulk

$\text{Cd}_{1-x}\text{Mn}_x\text{Te}$ [17]. In equation (9), ψ is the envelope function as given in equation (7) with the appropriate values of the variational parameters, k_B is the Boltzmann constant and $B_s(\eta)$ is the modified Brillouin function.

The parameters used in our calculations are $N_0 = 2.94 \times 10^{22} \text{ cm}^{-3}$, $\alpha N_0 \approx 220 \text{ meV}$, and the semi-phenomenological parameters $S_o(X_{in} = 0.02) = 1.97$, $S_o(X_{out} = 0.1) = 1.08$, $T_o(X_{in} = 0.02) = 0.94$, and $T_o(X_{out} = 0.1) = 3.84^{22}$. Using the envelop function given in equation (7) with the appropriate variational parameters, we obtain

$$E_{sp} = \frac{1}{2} \alpha N_0 [X_{in} S_0(X_{in}) I_1 + X_{out} S_0(X_{out}) I_2] \quad (12)$$

where

$$I_1 = \int |\psi_{in}|^2 B_s(\eta_1) d\tau, \quad I_2 = \int |\psi_{out}|^2 B_s(\eta_2) d\tau,$$

and

$$B_s(\eta_j) = \frac{2S+1}{2S} \coth\left(\frac{2S+1}{2S} \eta_j\right) - \frac{1}{2S} \coth\left(\frac{\eta_j}{2S}\right), \quad (13)$$

with

$$\eta_1 = \frac{S\alpha |\psi_{in}|^2}{2k_B[T + T_0(x_{in})]} + \frac{g\mu_B SB}{k_B[T + T_0(x_{in})]}$$

and

$$\eta_2 = \frac{S\alpha |\psi_{out}|^2}{2k_B[T + T_0(x_{out})]} + \frac{g\mu_B SB}{k_B[T + T_0(x_{out})]}.$$

3 Results and discussion

The estimated variation of barrier height with magnetic field by our extrapolated model for the case of donors in the diluted magnetic semiconductor $\text{Cd}_{1-x}\text{Mn}_x\text{Te}$ is given in Figure 1. The barrier height becomes zero for a critical field ~ 50 Tesla which corresponds to $\gamma = 2.7$. The experimental critical magnetic fields are for the acceptor problem [16, 22].

In Figures 2, 3 we have displayed the variation of the binding energy of the electron corresponding to the lowest level in the Dot for different magnetic and electric field strengths as a function of dot radius. We observe the following: The lowest binding energy (i) decreases as dot radius increases and approaches the bulk value for large dot sizes; (ii) decreases as the magnetic field increases up to a dot size $\sim 3a^*$; the trend reverses beyond this dot size. The crossings are the consequences of the variation of the barrier height due to magnetic field, which is the characteristic of DMS QDs; and (iii) does not show much variation with electric field up to a dot size $\sim 3a^*$, unlike in the case of a quantum well [23]. Beyond $\sim 3a^*$, the variation with

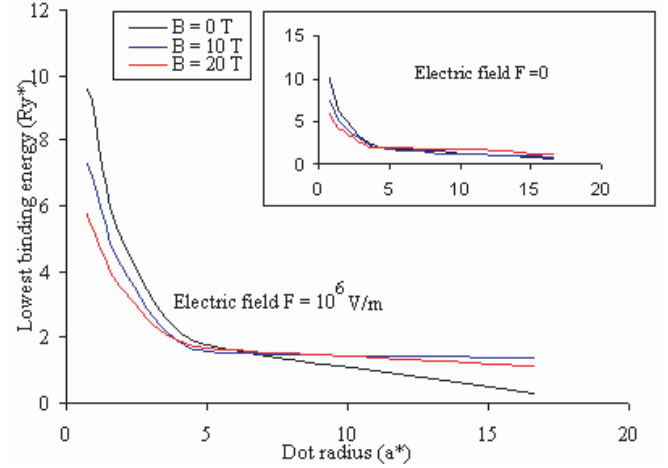


Fig. 2. Variation of lowest binding energy with dot radius for various magnetic and electric fields.

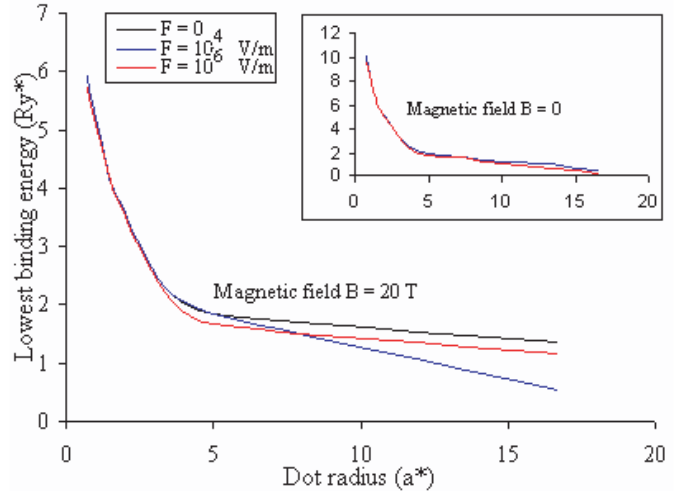


Fig. 3. Variation of the lowest binding energy with dot radius for various electric fields in the presence of a magnetic field.

electric field is as in the case of QW, as it is expected. In general, in all quantum well structures without magnetic elements (e.g. GaAs/GaAlAs systems) the magnetic field increases the binding energy [24]. In the present work, this situation is reversed which we believe is due to the reduction in barrier height in a magnetic field and the interplay between field induced localization and confinement due to V_0 . This situation is clearly brought out in Figure 4 where the lowest binding energy remains almost constant with the combined effects of both fields. The binding energy is higher for smaller dot radii due to the confinement, and the magnetic field effects are prominent for small size dots.

Donor ionization energy as a function of dot radius with different electric fields for a given magnetic field is shown in Figure 5. Donor ionization energy decreases in an electric field. The decrease is more for wider dots. As the electric field is increased the electron is pulled toward one side of the quantum dot as a result the binding energies decrease as a function of electric field for an on-center impurity. To bring about an appreciable change in the

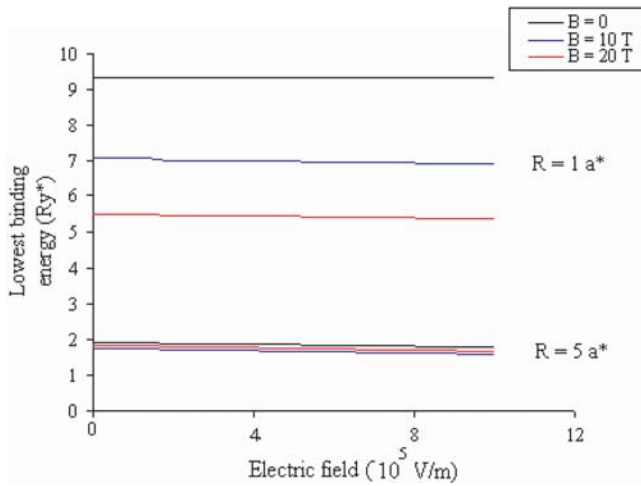


Fig. 4. Variation of the lowest binding energy with electric field for different dot radii. The upper set of lines indicates for the dot radius, $1a^*$ and the lower set of lines indicates for the dot radius, $5a^*$.

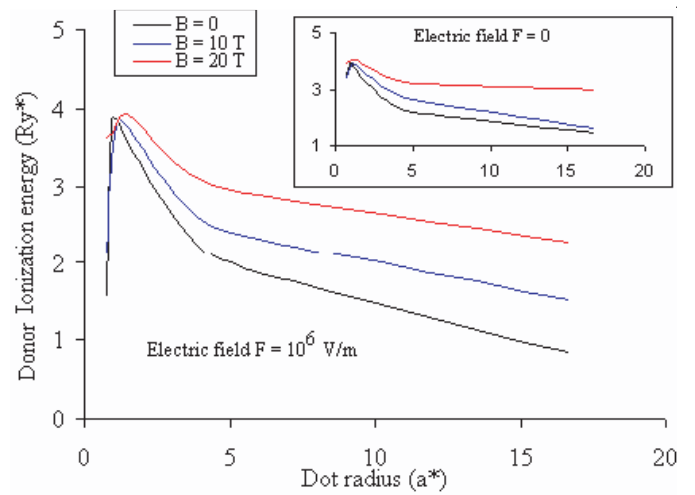


Fig. 6. Variation of ionization energy with dot radius for different magnetic fields in the presence of electric field. The inset shows the same without electric field.

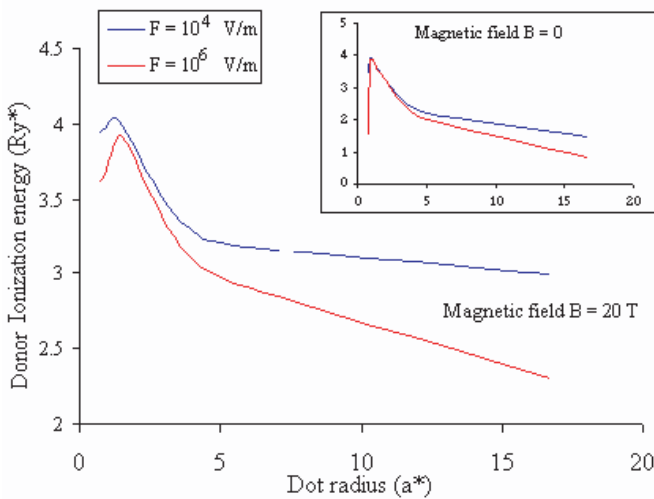


Fig. 5. Variation of ionization energy with dot radius for different electric fields in the presence of magnetic field. The inset shows the same without magnetic field.

donor ionization energy one has to apply a field of strength in excess of 1×10^6 V/m. It is also seen that for a given magnetic field, the ionization energy is reduced in an electric field.

The donor ionization energy as a function of dot radius, with different magnetic fields and a given electric field, is shown in Figure 6. As expected, the donor ionization energy decreases with an increase of dot radius, reaching the bulk value for large dot radii (see the inst in Fig. 6). Also we observe an increase in the donor ionization energy in a magnetic field. As the dot radius approaches zero the confinement becomes negligibly small, and in the finite barrier problem the tunneling becomes huge. The donor ionization energy again approaches the bulk value. Hence the variation of donor ionization energy with dot radius shows a peak around $1a^*$ for all the mag-

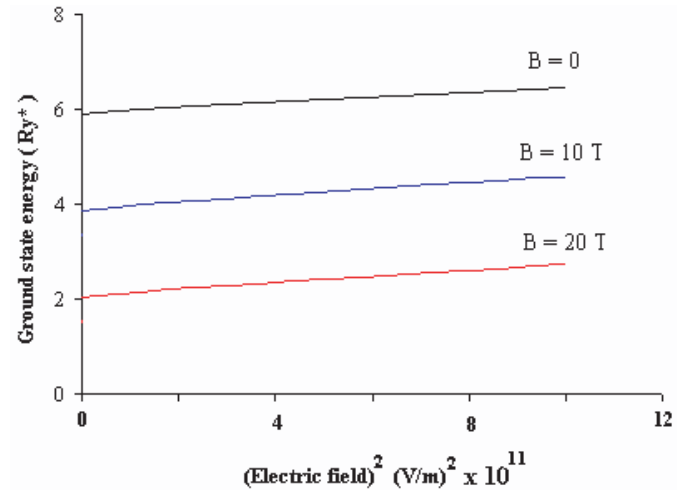


Fig. 7. Variation of ground state energy with the square of electric field strengths for the case of dot radius 55 \AA .

netic fields. This is a well known result in all quantum well structures [16]. Figure 6 also shows that the peak shifts to higher values of dot radius as the magnetic field increases indicating strong tunneling against localization.

In an attempt to estimate the donor polarizability we have plotted the ground state energy of the donor versus F^2 in Figure 7 for different magnetic fields. The slopes, namely $\partial \langle H \rangle_{\min} / \partial F^2$, for different magnetic fields give $-\alpha_{pol}/2$. The variation of polarizability with magnetic field is presented in Figure 8. The polarizabilities are estimated for three different dot radii, $R = 55 \text{ \AA}$, 100 \AA , and 200 \AA . The donor polarizability shows a peak around 10 T for a dot of radius less than a^* . Since the polarizability is derived from the energy, α_{pol} shows a peak as the energy does in Figures 5, 6. However, for $R \gg a^*$, α_{pol} does not show appreciable variation with magnetic field. The case of $R = 100 \text{ \AA}$ is interesting as the polarizability remains negative up to about 10 T and then increases. Such an

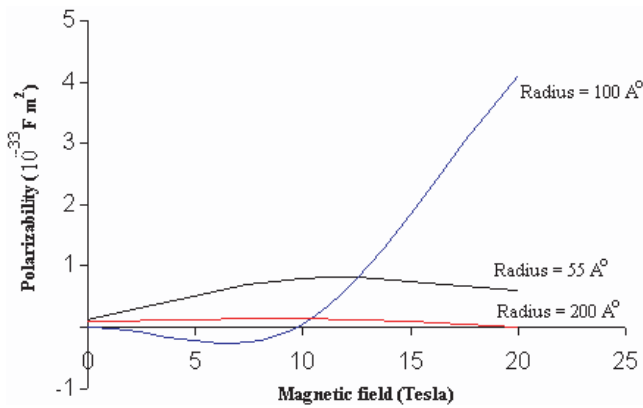


Fig. 8. Variation of polarizability with magnetic field.

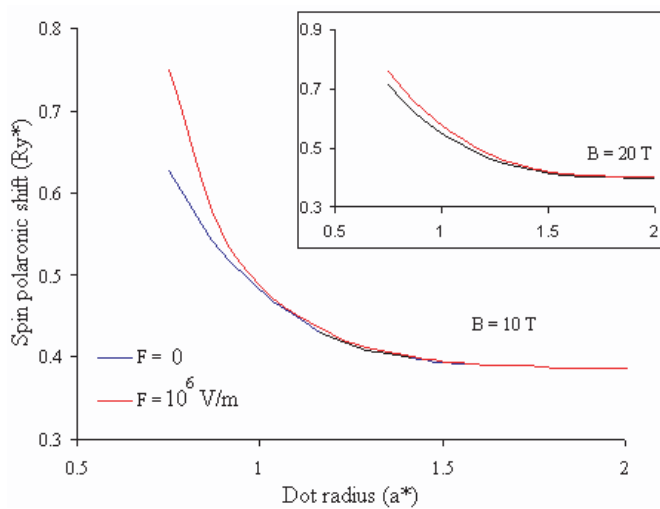


Fig. 9. Variation of spin polaronic shift with magnetic and electric fields for different dot radii.

anomalous behaviour is known for a quantum well system in an excited state [25]. This, we believe is a manifestation of non-linear effects in intense magnetic fields [26].

The increase of spin polaronic shift with magnetic field is clearly brought out in Figure 9. This figure also shows that for a narrow dot the polaronic effects are important as compared to a dot of large radius. For narrow dots the spin polaronic shift increases with electric field.

In this work, we have considered the effects of both electric and magnetic fields in the estimation of ionization energies of the donor in $\text{Cd}_{1-x_{in}}\text{Mn}_{x_{in}}\text{Te}/\text{Cd}_{1-x_{out}}\text{Mn}_{x_{out}}\text{Te}$ quantum dots. We have used the effective mass approximation within a variational procedure and for the first time, the cumulative effects of electric and magnetic fields applied along the growth direction of the system are discussed. We don't have at present sufficient experimental data to compare our results. However, the problem of a harmonic oscillator under a confined geometry has drawn the attention of several physicists like Landau, Fock and Darwin [27]. Since at present quantum dots are drawing more attention in areas like spintronics and quantum computers we hope that the present work will stimulate more experimental ac-

tivity on impurity states on quantum dots. Experimental efforts are encouraged to lend support to our calculations.

References

1. N. Porrás-Montenegro, S.T. Pérez-Merchancano, Phys. Rev. B **24**, 4714 (1981)
2. Shu-Shen Li, Kai Chang, Jian-Bai Xia, Phys. Rev. B **71**, 155301 (2005)
3. R.P. Taylor, R. Newbury, A.S. Sachrajda, Y. Feng, P.T. Coleridge, C. Dettmann, N. Zhu, H. Guo, A. Delage, P.J. Kelly, Z. Wasilewski, Phys. Rev. Lett. **78**, 1952 (1997)
4. D.K. Ferry, R. Akis, J.P. Bird, Phys. Rev. Lett. **93**, 026803 (2004)
5. C. Gustin, S. Faniel, B. Hackens, S. Melinite, M. Shayegan, V. Bayot, Phys. Rev. B **71**, 155314 (2005)
6. B.I. Halperin, A. Stern, Y. Oreg, J.N.H.J. Cremers, J.A. Folk, C.M. Marcus, Phys. Rev. Lett. **86**, 2106 (2001)
7. J.L. Zhu, J.J. Xiong, B.L. Gu, Phys. Rev. B **41**, 6001 (1990)
8. Z. Xiao, J. Zhu, F. He, J. Appl. Phys. **79**, 9181 (1996)
9. J.J. Vivas-Moreno, N. Porrás-Montenegro, Phys. Stat. Sol. (b) **210**, 723 (1998)
10. Corella-Maduene, R. Rosas, J.L. Martin, R. Reira, J. Appl. Phys. **90**, 5 (2001)
11. X. Liu, A. Petrou, D.D. McCombe, J. Ralston, G. Wicks, Phys. Rev. B **38**, 8522 (1988)
12. N.C. Jarosik, B.D. McCombe, B.V. Shanabrook, J. Comas, J. Ralston, G. Wicks, Phys. Rev. Lett. **54**, 1283 (1985)
13. B. Yoo, McCombe, W. Schaff, Phys. Rev. B **44**, 13152 (1991)
14. E. Ben Salem, S. Jaziri, R. Bennaceur, Phys. Stat. Sol. (b) **224**, 397 (2001)
15. Takahashi, K. Takabayashi, I. Souma, J. Shen, Y. Oka, J. Appl. Phys. **87**, 6469 (2000)
16. S.G. Jayam, K. Navaneethakrishnan, Int. J. Mod. Phys. B **16**, 3737 (2002)
17. J.A. Gaj, R. Planel, G. Fishman, Solid State Commun. **29**, 435 (1979)
18. F. Long, P. Harrison, W.E. Hagston, J. Appl. Phys. **79**, 6939 (1996)
19. H. Yokoi, S. W. Tozer, Y. Kim, D. Rickel, Y. Kakudate, S. Usuba, S. Fujiwara, S. Takeyama, G. Karczewski, T. Wojtowicz, J. Kossut, J. Appl. Phys. **85**, 5935 (1999)
20. M. Von Ortenberg, in *Applications of High magnetic field in Semiconductor Physics*, edited by G. Landwehr (Springer, 1983), p. 451
21. T. Kasuya, A. Yanase, Rev. Mod. Phys. **40**, 684 (1968)
22. K. Gnanasekar, K. Navaneethakrishnan, Mod. Phys. Lett. B **18**, 419 (2004)
23. G. Bastard, E.E. Mendez, L.L. Chang, L. Esaki, Phys. Rev. B **28**, 3241 (1983)
24. Zhigang Xiao, J. Appl. Phys. **86**, 4509 (1999)
25. D. Nguyen, T. Odagaki, Am. J. Phys. **55**, 466 (1987)
26. J. Frohlich, E.H. Lieb, M. Loss, Commun. Math. Phys. **104**, 251 (1986)
27. T. Chakraborty, *Quantum dots* (North Holland, Amsterdam, 1999)
28. E. Deleporte, J. M. Berroir, G. Bastard, C. Delalande, J. M. Hong, L.L. Chang, Phys. Rev. B **42**, 5891 (1990)
29. S. Kuroda, K. Kojima, K. Takita, K. Uchida, N. Miura, J. Cry. Growth **159**, 967 (1996)